Appl. Phys. A 31, 65–70 (1983)

Applied Physics A Solids and Surfaces

Electron Transport in Sub-Micron GaAs Channels at 300 K

B. R. Nag

Centre of Advanced Study in Radio Physics & Electronics, Calcutta University, Calcutta, India

M. Deb Roy

Physics Department, Jadavpur University, India

Received 8 February 1983/Accepted 7 March 1983

Abstract. Transient velocity-field characteristics have been computed for GaAs channels having lengths of 0.1, 0.2, 0.5, 1, and 20 μm for electric fields between 1 and 50 kV/cm at 300 K. The results are compared with earlier calculations and the significant features of the computed results are discussed. It is found that the electron motion for all channel lengths and for all fields is significantly affected by collisions. The threshold field for negative differential mobility increases, and the magnitude of the differential mobility decreases with decrease in the length of the sample. The maximum steady-state velocity increases with decrease in the length and may be as high as 5.4×10^7 cm/s for 0.1 μm samples.

PACS: 72.20, 72.60, 85.40

Gallium arsenide FET's with sub-micron channel lengths offer the possibility of realising picosecond-range low-power logic elements with power delay products of the order of femto-Joules [1]. Electron transport in such devices have, therefore, received extensive attention in recent years. The characteristics of such devices have been obtained using two different models. In one group of papers electrons are assumed to be injected from one end and the motion is assumed to be ballistic [2–17]. In early analyses, electrons were assumed to move without suffering any collisions and the current-voltage characteristics were found to be of the same nature as in vacuum tubes, but modified by the presence of ionized impurities. Effects of collision were later introduced phenomenologically using momentum and energy relaxation times and the corresponding balance equations. In the second group of papers [18–24] electron transport has been analysed by the Monte Carlo method assuming that electrons start with Maxwellian velocities corresponding to the lattice temperature at one end and move in a uniform electric field suffering collisions. Available experimental results are reported to be in agreement with the ballistic calculations [25, 3].

In an actual device, however, the electrons are initially uniformly distributed in the sample and start moving from different positions when the field is applied. Only as electrons reach the terminals and move out of the sample, new electrons are injected from the other end. In actual operating conditions, electrons may be removed even from the source end and injected from the drain end, although totally a larger number of electrons enter the sample from the source end and leave at the drain end. We have carried out Monte Carlo calculations of transient velocity-field characteristics at 300 K, taking into account the above considerations. The results are presented in this paper.

1. Method of Calculation

The electric field across the sample was assumed to be uniform as in the earlier Monte Carlo simulations. It was taken to be applied as a step and the position of the electron in the sample at the instant of application of the field and its velocity vector at that instant (according to Maxwell's distribution law corresponding to the lattice temperature) were first obtained by

Table 1. Values physical constants used for Monte Carlo simulation

Constant	Valley	Unit	Numerical value
Energy separation	$\Gamma-L$	eV	0.3
between valleys	$\Gamma-X$	eV	0.48
Effective mass of electron			
m_c^*, m_D^*	Γ	m_e	0.063
m_c^*	L	m_e	0.128
m_D^*	L	m_e	0.244
m_c^*, m_D^*	X	m_e	0.58
Intervalley phonon energy,	$\Gamma-L$	eV	0.0278
coupling constant		10^8 eV/cm	10
	$\Gamma-X$	eV	0.0299
		10^8 eV/cm	10
	$L-X$	eV	0.0293
		10^8 eV/cm	5
	$L-L$	eV	0.0290
		10^8 eV/cm	10
	$X-X$	eV	0.0299
		10^8 eV/cm	7
Non polar optic phonon energy,	L	eV	0.0343
coupling constant		10^8 eV/cm	3
Polar optic phonon energy	All	eV	0.03536
Static dielectric constant			12.90
Optical dielectric constant			10.92
Acoustic deformation potential	Γ	eV	7
	L	eV	2.24
	X	eV	3
Non-parabolicity factor	Γ	eV^{-1}	0.610
	L	eV^{-1}	0.461
	X	eV^{-1}	0.204
Velocity of sound		10^5 cm/s	5.24
Mass density		gm/cm^3	5.36
Lattice temperature		K	300

random numbers. The motion of an electron was then followed using the Monte Carlo procedure. The parameters of energy band structure and coupling constants for the various scattering mechanisms were taken to be the same as in Model C of Kratzer and Frey [21] (hereafter referred as KF). These are quoted in Table 1.

The component of velocity in the direction of the field was stored in the computer at intervals of 0.04 ps. It was assumed that as the electron reached the drain end it was removed from the sample and another electron with a lattice temperature Maxwellian velocity, determined by a random number, was introduced at the source end. When an electron hit the source within the simulation time, it was assumed that it was replaced by an electron with a Maxwellian velocity at the drain end [26, 27].

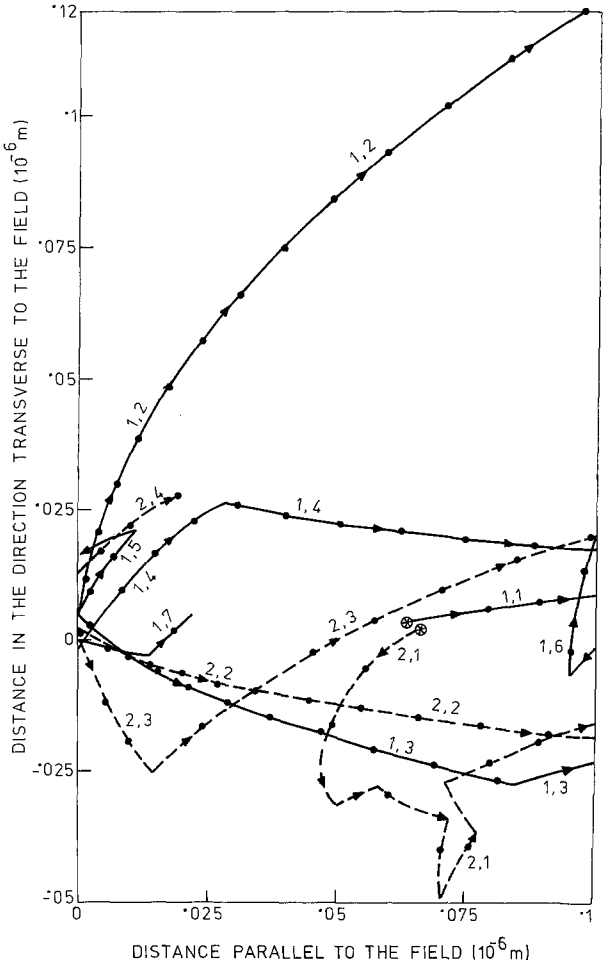

Fig. 1. Typical electron trajectories in 0.1 μm channel for a field of 10 kV/cm. The trajectories are numbered *a*, *b*; *a* indicates *a*th electron and *b* indicates the *b*th part of the trajectory of the *a*th electron

Figure 1 illustrates typical trajectories of two electrons. It is evident from these trajectories that the real situation is such that in course of motion the electron may start from the source end and reach the drain end as in ballistic motion, may suffer large number of collisions before reaching the end, may not reach the drain end or attain the ballistic maximum velocity. Earlier ballistic theory or the Monte Carlo simulations do not consider these complexities of the trajectories.

Velocity components were accumulated in our simulation for a few thousand electrons for different instants. The total current in the external circuit due to the electrons is

$$i(t)=\sum_{k=1}^{n} ev_k(t)/L, \tag{1}$$

where n is the number of sampled electrons, $v_k(t)$ is the velocity of the electron at time t after the application of

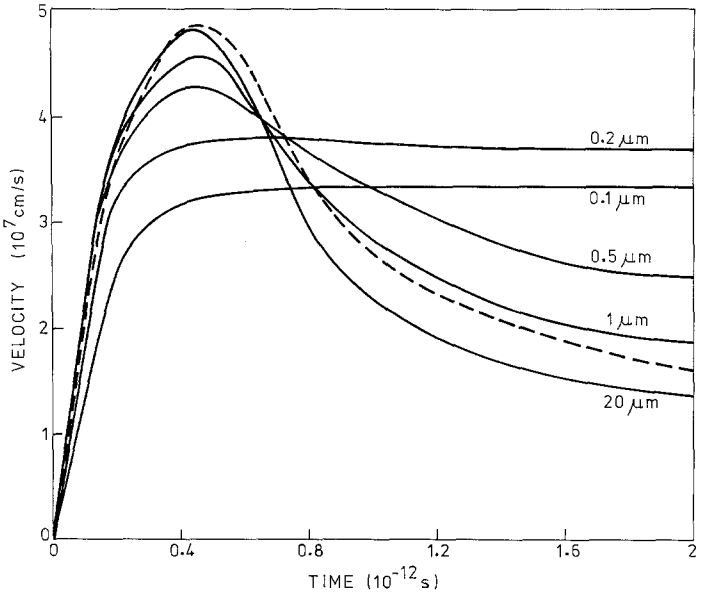

Fig. 2. Average electron velocity versus time for channels of different lengths with a field of 10 kV/cm. (Solid lines: present results, dotted line: Ruch's result)

the electric field, e is the electron charge, and L is the length of the sample. Hence $\sum_{k=1}^{n} v_k(t)/n$ is a measure of the current and we summed up at intervals of 0.04 ps for a total duration of 2 ps and obtained the average $\sum_{k=1}^{n} v_k(t)/n$ for every interval. Convergent results were obtained using about 2000 or more samples.

The average-velocity-time characteristics for 300 K obtained with the above procedure are presented in Fig. 2. Results are given for a field of 10 kV/cm for channel lengths of 0.1, 0.2, 0.5, 1, and 20 μm. We find that for small channel lengths upto about 0.2 μm the velocity monotonically increases with time and reaches a steady saturation velocity in about 0.4 ps. The number of electrons transferred to the upper satellite valley is insignificant. For larger channel lengths, on the other hand, the velocity rises to a peak value in about 0.4 ps and then decreases with time and reaches a steady value after about 1.5 ps. Substantial transfer of electrons to the higher valleys for these channel lengths starts from about 0.4 ps. The peak value increases while the steady state value decreases with increase in the channel length.

The general features may be understood considering that the average time for which the electrons are accelerated increases with the channel length and hence the steady-state velocity increases. However, as the length further increases, some electrons have sufficient time to acquire enough energy for transfer to higher satellite valleys, and as a result the velocity decreases. The fraction of electrons which are transferred to higher valleys increases with increase in the channel length. The steady-state velocity, therefore, decreases and approaches the bulk value with increase in the channel length.

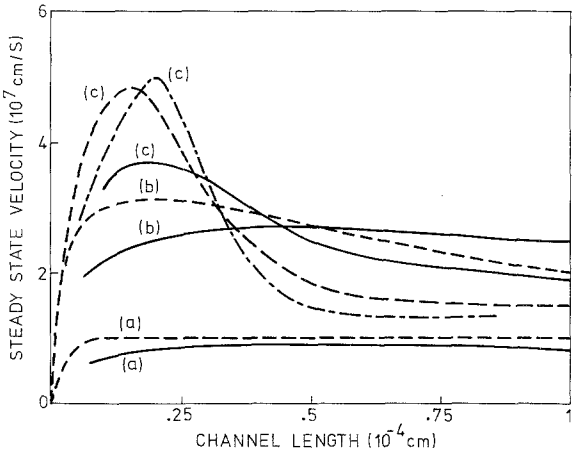

Fig. 3. Steady-state velocity versus channel length for fields of 1, 5, and 10 kV/cm. Solid line: present results, dotted line: Ruch's results, Dot-dash: Kratzer and Frey's results. (a) 1 kV/cm, (b) 5 kV/cm, (c) 10 kV/cm

Evidently, the results of our simulations would be identical to that of earlier Monte Carlo calculations for long channel lengths. The contribution of electrons starting near the ends may be considered negligible for such lengths. On the other hand, all the electrons starting away from the ends will have trajectories as if they were injected at one point. We have plotted in Fig. 2. Ruch's results [18] for comparison. It is seen that the initial part of the curve is almost identical to that for 20 μm lengths. Ruch's values for longer times are slightly higher which may be explained as being due to the difference in the values of the physical

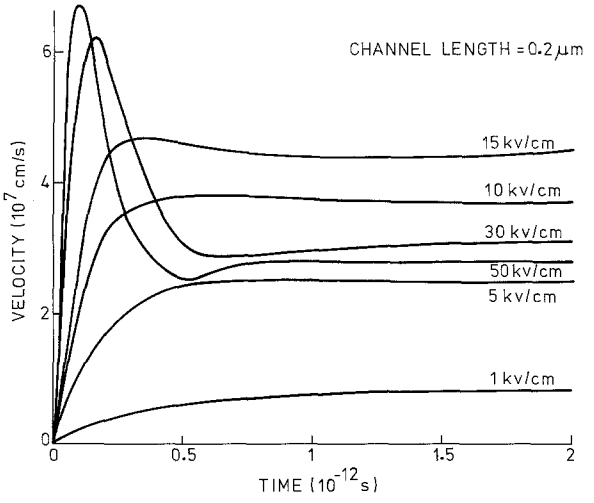

Fig. 4. Average velocity versus time for different fields (1–50 kV/cm) for a channel length of 0.2 μm

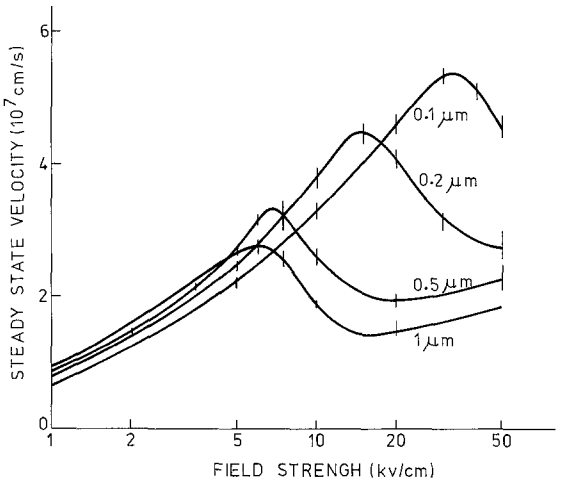

Fig. 5. Steady-state velocity versus field for different channel lengths

constants. Ruch's model and model C of KF differ in parameter values for higher valleys. Since we used KF's values, the curves for larger time, which are influenced by transfer to higher valleys may be expected to be different.

We compare in Fig. 3 the steady-state velocity for submicron channel lengths given by our model with the velocity-distance curves of earlier Monte Carlo calculations. It is seen that our results are significantly different for very small channel lengths. The discrepancy is understandable on considering the difference in the two models of calculations.

Our model is evidently more realistic and we applied it to explore in details the velocity-field relationships for sub-micron channel lengths. These results are presented below.

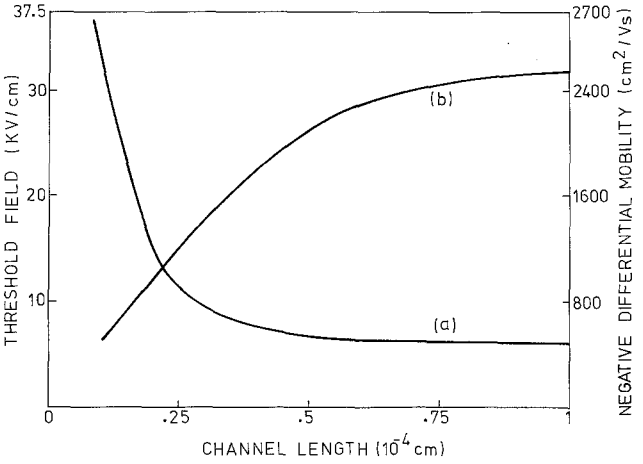

Fig. 6. Threshold field for negative differential mobility and its magnitude for different channel lengths. (a) Threshold field; (b) Magnitude of negative differential mobility

2. Transport Characteristics

We present in Fig. 4 velocity-time curves for a channel length of 0.2 μm and for fields from 1 to 50 kV/cm. It is seen that upto about 15 kV/cm, the curves have the same shape, the velocity rises monotonically to a saturation value with a rise-time which decreases with increase in the field. The value of rise-time for a field of 15 kV/cm is about 0.3 ps. Effects of electron transfer to higher valleys starts showing from a field of about 15 kV/cm. For higher fields the average velocity shoots up in about 0.15 ps and then decreases to a value lower than the steady state value for 15 kV/cm.

The general features that the steady-state velocity will increase with increase in the field and above a critical field the velocity will decrease with the field, are true for all the sample lengths. However, our simulations bring out a very important point that the value of the critical field above which the velocity-field characteristic shows a negative slope increases with decrease in the sample length. This feature is illustrated through the graphs presented in Figs. 5 and 6.

Figure 5 presents the velocity-field curves for different channel lengths. We find that a negative slope is obtained for 1 and 0.5 μm length at around 6 kV/cm. On the other hand, for 0.2 μm channel length, the negative slope appears around 12–15 kV/cm, whereas for 0.1 μm it occurs around 30–35 kV/cm. The magnitude of the negative slope also decreases with decrease in the channel length, as is evident from Fig. 6. These results are in agreement with the experiments on Gunn diodes [28] and leads to an important conclusion. The frequency limitation of such devices have been reported earlier to arise from the finite value of the various relaxation time constants. It was estimated that the

negative differential mobility will disappear from around 140 GHz [29]. We find from the present calculations that a size limitation of the operating frequency should also be considered important. A Gunn diode for a frequency of 100 GHz would have a length of about 1 μm. It is evident that any further reduction in length for realising higher-frequency diodes would not be fruitful as the operating field would be much higher and the negative differential mobility small.

We illustrate in Fig. 7, the variation of steady-state velocity with the channel length for different fields. It is seen that for any channel length there is an optimum field for realising the highest possible velocity. For channel lengths above 0.5 μm the highest attainable velocity is about 2×10^7 cm/s, whereas for smaller channel lengths much higher velocity may be attained. For a channel length of 0.1 μm the velocity for a field of 30 kV/cm is 5.4×10^7 cm/s. Our calculations could not be made extensive enough to cover all possible channel lengths and all fields. It is, however, established that for any channel length, there is an optimum field for realising the highest velocity and the highest frequency. This field increases and also the maximum velocity increases with decreasing channel length. The opterating frequency of a short channel FET will thus increase much faster than the inverse of the length.

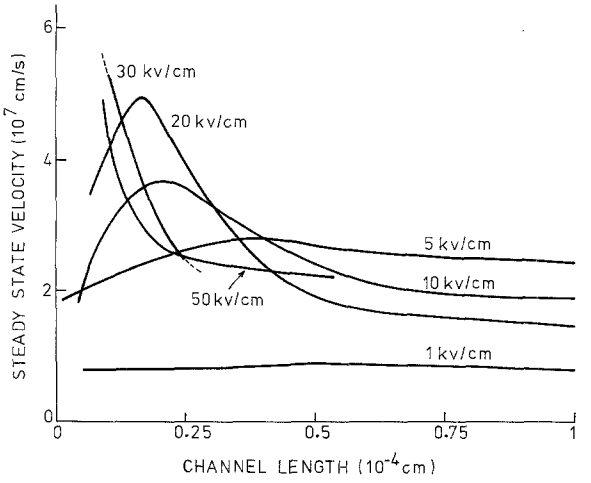

Fig. 7. Steady-state velocity versus channel length for different fields

3. Kinetics of Electron Motion

We find from Fig. 5 that the velocity-field characteristics given by our model are significantly different from those given by the ballistic analysis. It should be noted that for the initial part of the velocity-time curve our model would give results very different from those given by earlier models. However, for the steady state, as mentioned earlier, the electrons drift out of the sample at the drain end and the motion of electrons

Table 2. Characteristic parameters of electron trajectories

Field [kV/cm]	Channel length L [μm]	Average transit time [ps]	Average number of collision per sample		Number of crossings per sample in 2 ps		Fraction in the upper valley	Steady state velocity [10^7 cm/s]
			[2 ps]	Per transit	At $x=0$	At $x=L$		
1	0.1	1.3	8.75	5.7	1.35	2.6	0.0005	0.75
	0.2	2.4	8.95		0.73	1.44	0.0005	0.82
	0.5	5.7	9.24		0.32	0.60	0	0.87
	1.0	11.9	9.23		0.016	0.031	0	0.84
5	0.1	0.45	10.33	2.3	0.78	4.98	0.0005	2.2
	0.2	0.8	11.23	4.5	0.44	2.78	0.0005	2.5
	0.5	1.8	12.37	11.1	0.17	1.21	0.013	2.7
	1.0	3.7	13.06		0.092	0.63	0.071	2.7
10	0.1	0.3	12.3	1.8	0.52	6.7	0.01	3.35
	0.2	0.53	13.7	3.6	0.32	3.93	0.011	3.74
	0.5	1.88	20.8	19.5	0.11	1.32	0.173	2.66
	1.0	5.3	24.1		0.053	0.60	0.506	1.89
20	0.1	0.22	14.62	1.61	0.365	9.37	0.01	4.6
	0.2	0.48	23.17	5.56	0.177	4.37	0.25	4.2
	0.5	2.78	39.5		0.041	0.92	0.69	1.8
	1.0	7.14	41.9		0.024	0.44	0.74	1.4
30	0.1	0.18	17.4	1.56	0.312	10.8	0.059	5.42
	0.2	0.62	39.7	12.3	0.097	3.39	0.54	3.1
50	0.1	0.22	35.88	3.95	0.16	9.54	0.37	4.6
	0.2	0.74	63.44	23.47	0.05	3.07	0.69	2.7

replacing them from the source end should be similar to those in the ballistic model for a uniform field distribution, i.e., the average velocity for a particular channel length should vary as the square root of the field-length product. Our results being very different, it would appear that even for a channel length of 0.1 μm, the ballistic model is not applicable. In order to have a better understanding of the kinetics of electron motion we recorded, along with the velocity-field characteristics, a number of characteristic parameters of motion. These are listed in Table 2.

It is seen from Table 2 that for all the channel lengths and at all the fields, electrons suffer collisions. The number of collisions first decreases, attains a minimum and increases again with increase in the field. The number of collisions, as expected, increases also with increase in the channel length. We also find an important feature that a significant fraction of electrons leave the sample at the source end for small channel lengths and at low fields. This fraction decreases with increase in the field. It appears from these results that the kinetics of electron transport for small fields is very much of the nature of collision-dominated conduction motion even for small channel lengths. The kinetics changes to that of the ballistic type at high fields. But, for all fields the collisions have significant effects. The ballistic model, therefore, is not likely to be applicable at 300 K for describing the electron motion even in devices with a short channel of 0.1 μm length. Also, as the number of collisions is not large, the phenomenological analysis using average momentum and energy relaxation times is not very appropriate. The velocity-field characteristic is likely to correspond, in general, to a mixed conduction (collision dominated) and ballistic motion.

We should note that although our calculations bring out the significant features of electron transport in short channels, a straightforward comparison with experiments would not be very meaningful. In a practical device the field and the electron distribution would not be uniform and terminal conditions may also be different [30]. Some of the general features of the characteristics found from our analysis may only be qualitatively verified by performing experiments on devices with different channel lengths. Experimental results of Hollis et al. [31] show a quasi-linear relationship between current and voltage for a 0.24 μm long channel at 300 K which, however, is not in agreement with our results.

4. Conclusion

Transient velocity-field characteristics of submicron length GaAs channels have been computed for 300 K using a new model of Monte Carlo calculations.

It is found that the critical field for negative differential mobility increases whereas the magnitude of the mobility decreases with the channel length.

There is an optimum field for which the steady-state velocity is maximum for any channel length. The maximum velocity for very short channels may be 3 times the bulk saturation velocity. The transit time is found to decrease much faster than the inverse of the length.

A detailed analysis of the kinetics of electron motion indicates that the motion is significantly affected by collisions for channel lengths as short as 0.1 μm at all fields. The motion is of the mixed (conduction and ballistic) type.

References

1. H. Rees, G.S. Sanghera, R.A. Warriner: Electron. Lett. **13**, 156 (1977)
2. M.S. Shur, L.F. Eastman: IEEE Trans. ED-**26**, 1677 (1979)
3. M.S. Shur, L.F. Eastman: Electron. Lett. **16**, 522 (1980)
4. J.B. Socha, G.J. Rees: Electron Lett. **16**, 872 (1980)
5. K. Hess: IEEE Trans. ED-**28**, 937 (1979)
6. J. Lee: J. Appl. Phys. **52**, 4676 (1981)
7. J.R. Barker, D.K. Ferry, H.L. Grubin: IEEE Electron Dev. Lett. EDL-**1**, 209 (1980)
8. M.S. Shur, L.F. Eastman: IEEE Electron Dev. Lett. EDL-**1**, 147 (1980)
9. M.T. Elliot, M.P. Splinter, A.B. Jones, J.P. Reekstin: IEEE Trans. ED-**26**, 469 (1979)
10. R. Zuleeg: IEEE Electron Dev. Lett. EDL-**1**, 234 (1980)
11. M.S. Shur: IEEE Trans. ED-**28**, 1120 (1981)
12. M.S. Shur: Electron. Lett. **12**, 615 (1976)
13. D.K. Ferry, J.R. Barker: Solid State Electron. **23**, 545 (1980)
14. R.S. Huang, P.H. Ladbroke: J. Appl. Phys. **48**, 4791 (1977)
15. M.S. Shur, L.F. Eastman: Solid State Electron. **24**, 11 (1981)
16. W. Frensley: IEEE Electron. Dev. Lett. EDL-**1**, 137 (1980)
17. J.P. Nougier, J.C. Vaissiere, D. Gasquet, J. Zimmermann, E. Constant: J. Appl. Phys. **52**, 825 (1981)
18. J.G. Ruch: IEEE Trans. ED-**19**, 652 (1972)
19. T.J. Maloney, J. Frey: IEEE Trans. ED-**22**, 357 (1975)
20. T.J. Maloney, J. Frey: J. Appl. Phys. **48**, 781 (1977)
21. S. Kratzer, J. Frey: J. Appl. Phys. **49**, 4064 (1978)
22. M. Brauer: Phys. Status Solidi (b) **81**, 147 (1977)
23. G. Hill, P.N. Robson, A. Majerfeld, W. Fawcett: Electron. Lett. **13**, 235 (1977)
24. Y. Awano, K. Tomizawa, N. Hashizume, M. Kawashima: Electron. Lett. **18**, 133 (1982)
25. L.F. Eastman, R. Stall, D. Woodard, N. Dandekar, C.E.C. Wood, M.S. Shur, K. Board: Electron. Lett. **16**, 524 (1980)
26. J. Zimmermann, E. Constant: Solid State Electron. **23**, 915 (1980)
27. R. Fauquembergue, M. Punisek, E. Constant: Electron. Lett. **18**, 671 (1982)
28. D.P. Brady, S. Knight, K.L. Lawley, M. Uenohara: Proc. IEEE **54**, 1497 (1966)
29. H.D. Rees: Solid State Commun. **7**, 267 (1969)
30. J.J. Rosenberg, E.J. Yoffa, M.L. Nathan: IEEE Trans. ED-**28**, 941 (1981)
31. M.A. Hollis, L.F. Eastman, C.E.C. Wood: Electron. Lett. **18**, 570 (1982)